University of
Strathclyde
Engineering

Department of Mechanical and Aerospace Engineering

Blue Hydrogen: Modelling the Efficiency of a Steam Methane Reformer

Author: Scott Griffin

Supervisor: Cameron Johnstone

A thesis submitted in partial fulfilment for the requirement of degree in

Master of Science in Sustainable Engineering: Renewable Energy Systems and the Environment

2022

Student No. 202169976

Copyright Declaration

Abstract

A steam methane reforming (SMR) plant was modelled on MATALB to observe the effects of various design factors on the overall efficiency of the system. As the majority of energy input to an SMR system is during the reformer stage, the analysis focused on the design factors of the reformer. Using yield values and design parameters taken from SMR studies, the efficiency was calculated by considering heat loss, frictional head loss, fuel consumption, and compressor work, with a requirement of at least 1 second of contact time for the process fluid in the reformer pipes. At baseline conditions, the system had an efficiency range of 48.03-58.68%, with a contact time of 2.6 seconds. A sensitivity analysis was then undertaken to examine the effects of pipe length, pipe diameter, mass flow rate, and the number of pipes used in the reformer. Determining the correlations between these variables and the system efficiency, the model was run with five additional sets of design parameter in order to maximise the efficiency. The maximum efficiency achieved while keeping the contact time above 1 second was 64.14% at a contact time of 1.22 seconds.

Student No. 202169976

Acknowledgements

I would like to express my appreciation to my project advisor Cameron Johnstone for providing key advice and discussion throughout the process of this project.

I would also like to thank my family for providing much support throughout my time at university.

Student No. 202169976

Table of Contents

Student No. 202169976

List of Figures

List of Tables

Student No. 202169976

Nomenclature

ATR – Autothermal reforming

GHG – Greenhouse gas

GWP – Global warming potential

PSA – Pressure swing absorption

SMR – Steam methane reforming

WGS – Water-gas shift

1.0 Introduction

With efforts to minimise greenhouse gas emissions in the energy sector through ambitious net zero targets by 2050, there is a large demand to adopt new low-emission energy production methods. As fossil fuels make up a substantial majority of the world's energy production (84% in 2019) [1], a key aspect is to provide power sources capable of providing the quantities of energy which fossil fuels currently supply. The leading alternatives which have to take over the demand created from a fossil fuel phase-out are nuclear energy and renewable energy. Both of these sources have their own intricacies and arguments, but they are both advantageous in terms of emissions when compared to fossil fuels. These technologies have been given a large focus over the last decade, with renewable sources being scale up by around 247% between 2011 and 2021 [2]. Over the last several years, however, hydrogen technology has been pushed as another alternative to fossil fuels.

Hydrogen gas has a high energy density, meaning that it contains high amount of energy per unit mass, relative to other sources. Although hydrogen is the most common element in the universe, the process of separating H_2 molecules from other element provides technical challenges for producers. There are two main methods which hydrogen can be produces; the electrolysis of water and the reforming of natural gas, which is most commonly done by steam methane reforming (SMR). The electrolysis of water is known as green hydrogen as it is the only products from the process are hydrogen and water (no emission). The reformation of natural gas, when combined with carbon capture technology is referred to as blue hydrogen.

Green hydrogen is the preferred long-term technology as it provides less emissions than blue hydrogen, large scale commercial electrolysis is still in its infancy and therefore a very expensive process. While blue hydrogen still emits greenhouse gases, much of the infrastructure already used in the natural gas industry can be repurposed to suit blue hydrogen technology, therefore, blue hydrogen is considered a key opportunity to scale down fossil fuel reliance and develop a hydrogen economy while green hydrogen is still maturing. It is for this reason that the UK hydrogen strategy has an emphasis on blue hydrogen with a planned total of at least 900 MW of blue hydrogen production compared to a total of around 150-200 MW of green hydrogen production [3].

The aim of this study is to mathematically model the reformer of an SMR plant to determine the design factor associated with the overall efficiency of the system.

2.0   Literature Review

2.1 Steam Methane Reforming

SMR is currently used to produce a large majority of the world's hydrogen. There are four main steps to the steam reforming of natural gas, the first being the pre-treatment of the natural gas feed. The catalysts used in the reforming stage are highly sensitive to sulphur and therefore before this stage all sulphur compounds present in the natural gas must be removed. A common method of removing sulphur is to first hydrogenate it by introducing recycled H_2 to the feed, which forms hydrogen sulphide (H_2S). The feed is then sent through a bed of zinc oxide (ZnO), which reacts with the hydrogen sulphide to form zinc sulphide (ZnS) [4].

After the feed has been through pre-treatment it is mixed with steam sent through the reformer. The steam for this process is generated in heat exchanger with the high-temperature mixture from the reformer tubes and the output heat from the burners. The reformer consists of catalyst-packed tubes, usually made of nickel, where the natural gas and steam mix is sent through. Outside of these tubes are burners which combust natural gas and flue gas from which was rejected at a later stage of the process. The burners heat the process gas inside the tubes to temperatures between 800-1000°C and pressures of 14-20 bar where the methane and natural gas mixture forms into carbon monoxide and hydrogen in an endothermic reaction (*equation 2.1*) [5].

$$CH_4 + H_2O \leftrightarrow CO + 3H_2 \quad \Delta H^0_{298} = 206.2 \; kJ/mol \qquad \textbf{(2.1)}$$
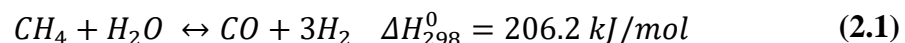
The products of this reaction are then fed into a water gas shift (WGS) reactor to increase hydrogen production and reduce CO content. The remaining carbon monoxide reacts with more steam to produce hydrogen and CO_2 (*equation 2.2*). As this reaction is exothermic it favours lower temperatures, however, high temperatures are desired for an appropriate reaction rate, therefore, this phase is usually split into a high temperature stage (around 300-450°C) and then a low temperature stage (200-250°C). the mixture for each phase of this stage is cooled using heat exchangers which are used to generate the steam for the reforming stage. There are several options for catalysts in this reaction; for high-temperature shift, iron, chromium or copper can be used, and for low-temperature shift, copper, zinc or aluminium can be used [4] [5].

$$CO + H_2O \leftrightarrow CO_2 + H_2 \quad \Delta H_{298}^0 = -41.2 kJ/mol \tag{2.2}$$
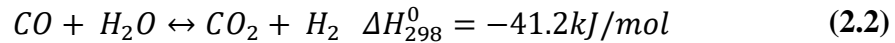
Combining *equations 2.1* and *2.2*, the overall reaction of the process is:

$$CH_4 + 2H_2O \leftrightarrow CO_2 + 4H_2 \quad \Delta H_{298}^0 = 165 \, kJ/mol \tag{2.3}$$
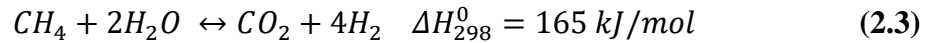
As hydrogen applications require high purity, the hydrogen must be separated from the remaining gases and steam using a pressure swing adsorption (PSA) system. The system consists of two pressurised tanks, both containing a bed of adsorbent material. The mixture is sent through one of the tanks where pressure builds, and the impurities stick to the material. When this tank is full the pure hydrogen is extracted, and simultaneously, the impurities are discarded while more mixture is fed into the second tank. The operation of each of these tanks works in tandem, where, when one tank is depressurising, the other is pressurising. This ensures a constant flow of hydrogen [6].

2.2 How Green is Blue Hydrogen

Some critics of blue hydrogen believe it to be more damaging than advertised and is a convenient way for natural gas providers to be able to continue exploiting fossil fuels. A peer reviewed research paper was published in 2021, which details the lifecycle emissions for blue hydrogen production, accounting for carbon dioxide, and unburned fugitive methane [7]. The paper's finding indicate that blue hydrogen is not a low carbon form of energy generation, particularly due to the associated methane emissions, which are commonly presented in a flawed manner, to give blue hydrogen a greener appearance. Calculating the global warming potential (GWP) of greenhouse gases (GHGs) is done in a set timeframe. As CO_2 has a long "half-life" in the atmosphere, its effects are typically calculated over a 100-year period. Similarly, the GWP of methane is commonly calculated on a 100-year basis, however, the half-life of methane is the atmosphere, is only around 12 years, therefore, when comparing the damage of methane to that of carbon dioxide across 100 years, its effects are overshadowed. This paper, however, calculated the GWP across a 20-year timeframe and find that methane is 86 times more impactful than CO_2 across this timeframe, on a mass-to-mass basis. The study also assumes a methane emission rate of 3.5% throughout the entire process, which is verified through 20 different studies across several US natural gas fields.

Surprisingly, the baseline analysis of the study finds that the total emissions of blue hydrogen are only 9-12% smaller than that of grey hydrogen, while assuming a generous 85% carbon capture rate. The reason for such a small difference is because, as the authors note, the process is of carbon capture and storage is most commonly powered by the additional burning of natural gases, which offsets the number of emissions being avoided by the carbon capture process itself. The paper also compares the emissions of both grey and blue hydrogen to traditional fossil fuels, finding that while blue hydrogen emits the least CO_2, its associated methane emissions make it more environmental impactful per megajoule (shown in *figure 1*).
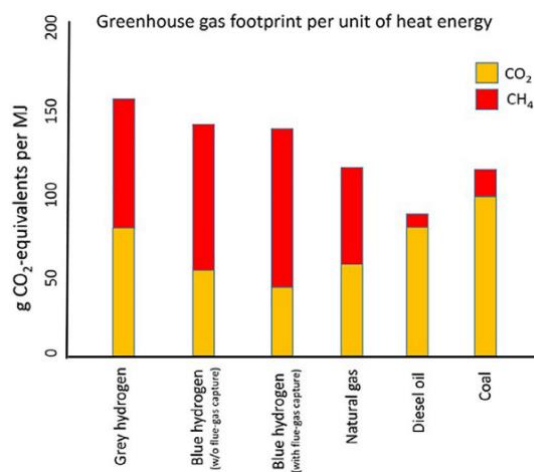
Figure 1: Emission results evaluating blue hydrogen against traditional natural gas sources [7]

The paper also suggests that "greenhouse gas footprint of blue hydrogen is more than 20% greater than burning natural gas or coal for heat and some 60% greater than burning diesel oil for heat" as there is more natural gas demand to generate and equivalent heat from hydrogen. Other considerations to take away from this study is that it assumes that CCUS allows carbon to be stored indefinitely which hasn't been proven at commercial scale. Furthermore, carbon the carbon stored from CCUS technology is typically used for oil recovery, which encourages further reliance on fossil fuels.

While carbon dioxide is often the focus when making efforts to slow the rate of climate change, as it is considered the worst form of emissions, this paper emphasises how important it is to limit other GHGs. Additionally, the paper points out the major flaw in the way that many companies measure the impact of methane emissions, by looking at it in the long-term instead of the short-term. A global methane assessment was published by the UN in 2021 and states that "global methane emissions must be reduced by between 40–45 per cent by 2030 to

achieve least cost-pathways that limit global warming to 1.5°C" [8]. With this target in mind, it makes much more sense to measure the effects of methane in a short-term.

This study has, however, been criticized over the assumptions made for its calculations. A paper was published in 2022, which aimed to address the shortcomings of this report [9]. A criticism by this paper is that the original study did not consider waste heat recovery in their analysis. Heat recovery is an important area for such a high temperature process like SMR, as it reduces energy consumption, not just for the sake of efficiency, but also to reduce emissions from heat energy generation. With this not being assumed, the energy input to the SMR system would result in an overestimation, by the standards of modern systems. The other main criticism this paper makes is that the original study takes its values of methane leakage and carbon capture efficiency from first-of-a-kind SMR plant which are not optimised for carbon and methane capture, as they were built when there was no demand or financial benefit to do so. With this in mind it can be determined that these values used in the study are on the high end of the spectrum, as the second paper states " …the range of estimated direct methane emissions across the supply chain is very large: from 0.2% to 10% of produced methane… the majority of the estimates lie between 0.5% and 3% of produced methane, with the mean across the estimates at 2.2%, and the median at 1.6%". This contrasts the value of 3.5% assumed in the original study.

The paper then calculates the emissions using the values from two studies on modern reforming plants which account for carbon capture and compares them to the finding of the original paper as well as the emissions from a regular methane burning plant. A segment of this analysis is shown in *figure 2.*
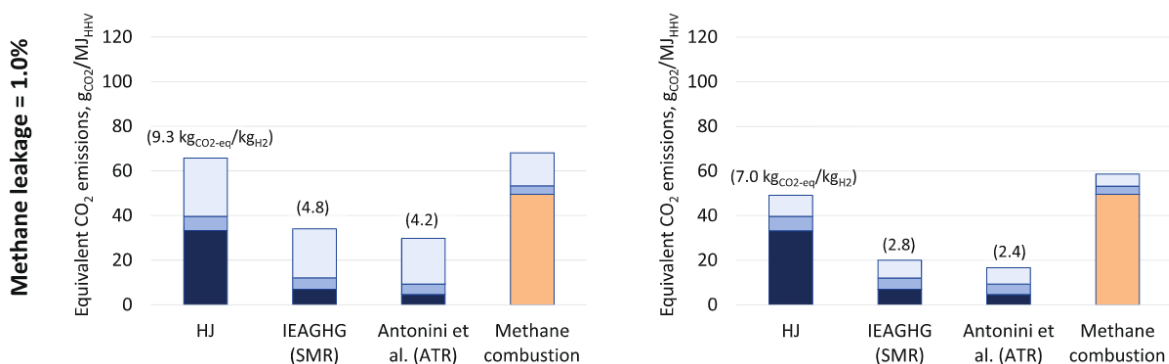
Figure 2: Results from emissions analysis, where HJ is the results from the original study [9]

Figure 1 shows the results with an assumed methane leakage rate of 1% at GWP values of 20 (left) and 100 (right). As shown the emission calculated for the sources used in this paper are smaller than that of the original by an average of 51.6% smaller for a GWP of 20 and 62.9%. As their results show, the criticisms made in this paper are reasonable and the comparison of emission to a tradition methane plant, would suggest that blue hydrogen could be considered a good intermediary step to scaling up the utilisation of hydrogen technology during the phase-out of fossil fuels. That being said, the point raised on the original paper in regard to measuring GWP on a 20-year basis is a relevant argument. There is a noticeable demand by industry members to follow this practice as in 2019 the state of New York mandated that methane GPW should be analyses on a 20-year basis [10]. Overall, the emissions of blue hydrogen should be assessed rigorously at both 100 and 20-year GWPs to give shareholders and industry experts full transparency.

2.3 Carbon Capture

Carbon capture technology is a vital area for blue hydrogen as its efficiency directly affects its level of emissions. There are three main methods of carbon capture in a natural gas plant.

2.3.1   Post-combustion

Post-combustion captures carbon from the flue gas which has been burned in the reformer. This is the easiest method of carbon capture to implement as it requires the least changes to an existing plant, which is a key element to consider since many new blue hydrogen plants will rely on pre-existing infrastructure [11]. The post-combustion option does, however, have limitations since the flue gas from combustion has a low CO_2 concentration (below 15%) and has a low partial pressure, meaning that the process is less efficient than the others [12].

2.3.1   Pre-combustion

This process can also be done before combustion. As the tail gas from the purification stage of a steam methane reforming process is used as fuel for the burners of the reformer, pre-combustion relies on capturing the carbon from the gas before it is burned. The capture of CO_2 typically takes place from the syngas after CO has been converted into CO_2 in the water-gas shift reactor, but in an SMR process, it is also common for the capture to take place after the purification stage. This is considered a very efficient process compared to post-combustion as the CO_2 concentration in the flue gas stream and the partial pressure of the

CO_2 is higher, making its extraction easier. Pre-combustion systems, however, do require a high capital cost and is difficult to retrofit in existing plants [13].

2.3.2 Oxyfuel-Combustion

Oxyfuel-combustion involves modifying the combustion chamber so that the fuel gas is burned in almost pure oxygen (around 97%) instead of air. By separating most of the nitrogen and argon from the air used in the combustion, the flue gas has a much larger concentration of CO_2. Before the combustion chamber the air goes through an air separation unit to obtain the high purity oxygen. The flue gas from this process mostly consists of CO_2 and steam which can be removed using a condensation unit. Additionally, the flue gas can be treated further to remove any remaining oxygen as well as contaminants caused by the small amount of remaining nitrogen and argon. Because of the air separation this process lowers the number of other pollutants such as NOx emitted. This method of capture, however, is also considerably expensive, mainly because of the air separation stage which uses a very energy intensive cryogenic distillation process. Like pre-combustion systems, oxyfuel-combustion is also difficult to retrofit in existing plants. Additionally oxy-combustion is a newer technology than the other two, therefore, further demonstration at industrial-scale me be required for it to be frequently adopted [14].

2.4 Reformer

The most common type of reformer is top fired, where fuel is combusted in burners on the outside of the process gas pipes and flows parallel to the mixture to heat it. These pipes are packed with catalyst particles, typically nickel based such as NiO/Al_2O_3. To expose the mixture to a high surface area of the material. The fuel used in the reformers is a mixture is the flue gas from the outlet of the PSA unit. This mixture contains some hydrogen and methane that has not been removed from the purification stage, though often more of these gases are added to ensure sufficient combustion. This mixture is then mixed with air and burned outside of the tube walls. Shown in *figure 3* is a diagram of a reformer showing the inputs and outputs.
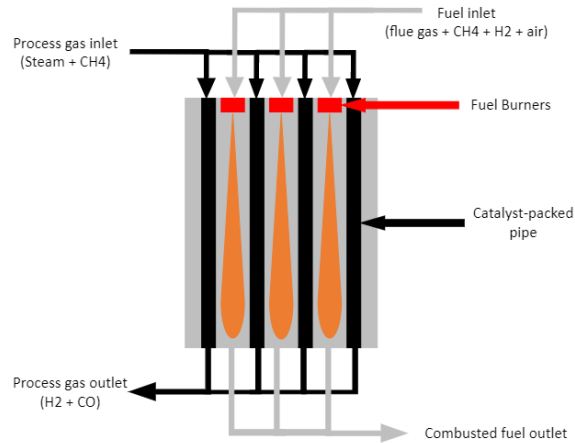
Figure 3: Diagram of top fired steam methane reformer

The process gas mixture enters the reformer around 600°C and exits around 800°C and the fuel can combust at around 1100°C [15]. Reformer walls are made of refractory metals with a low thermal conductivity to limit heat loss. The pipes in reformers are usually made of steel with a higher thermal conductivity than the refractor walls, so as to allow heat transfer from the combusted fuel to the process fluid.

As the reforming stage is an SMR plant is a catalytic process, time is required to allow the process mixture to completely react with the catalyst to ensure maximum hydrogen yield. Available literature for this required contact time was limited, however, one study suggests that conventional reformers require at least 1 second of a complete reaction. This paper focuses on microchannel reactors, experimenting with them at smaller contact times and concluded that high methane conversion was achievable at 900 µs with this design [16].

3.0   Method

According to a 2007 paper which conducts an exergy analysis on a steam methane reforming system, the majority of energy input into an SMR plant comes from the methane input to the system as a result of its heating value [17], meaning the overall efficiency of the plant is mostly affected by the reforming process and therefore, the focus of this analysis was on the reformer. A steady-state model reformer was developed using MATLAB and the results were recorded on Excel. The MATLAB code is shown in *Appendix 1*.

The hydrogen yield of the SMR plant was given by three papers as a ratio of moles per mole of methane in the process fluid. This number is influenced by the steam-to-methane ratio of the process gas (S/C ratio). Using these values, shown in *table 1*, the mass flow rate of each of these components could be calculated.

Table 1: S/C ratios and hydrogen yield for each case used in the analysis

S/C ratio (moles$_{H2O}$/moles$_{CH4}$)	Hydrogen yield (moles$_{H2}$/moles$_{CH4}$)	Source
3.2	2.25	[17]
3	2.47	[18]
3	2.7	[19]

In addition to the methane used in the process stream to produce hydrogen, methane is also used in the fuel that is combusted in the furnace section of the reformer in order to heat the mixture to the appropriate temperature. As well as this, hydrogen is used in the fuel mixture for combustion. The amount of fuel used in this process has an effect on the overall efficiency of the process, so the required amount of fuel to heat the furnace was determined with heat loss calculations. These calculations consider the conductive and convective heat transfer from the furnace area of the reformer to both the fluid in the pipes and the outside of the furnace area through the reformer walls. As the heat loss rate to both of these areas is a function of the reformer's geometry, a configuration was selected by consulting online study's which conduct modelling and CFD analysis of steam methane reformers. Referring to these studies also provided key operational parameters required for the analysis, such as temperatures and flow rates at different points of the system.

3.1 Geometry

The baseline conditions of the reformer geometry were taken from a the CFD modelling paper [15]. A topside view of the initial reformer design used is shown in *figure 4*. While the number of pipes pictured in *figure 4* is less than the actual amount used, the dimensions of the pipes from each other and from the reformer walls are consistent throughout the model.
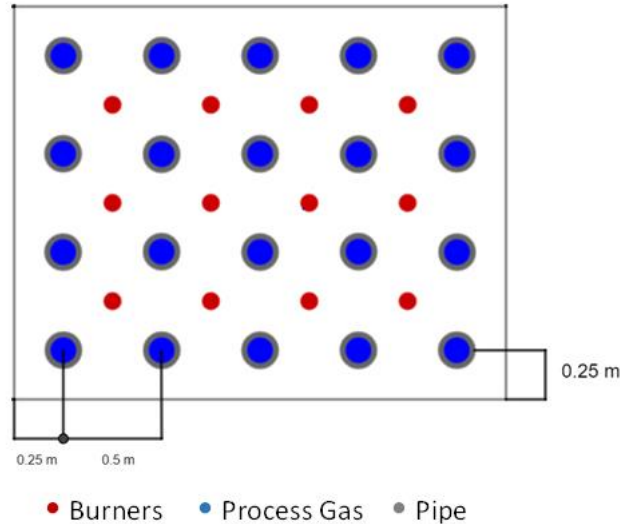
Figure 4: Diagram showing the top-down view of a reformer

These measurements were used to calculate the surface area of the reformer to account for heat loss.

$$Width = (diameter(number\ of\ pipes\ in\ a\ row))$$
$$+ (0.5(number\ of\ pipes\ in\ a\ row - 1) + (0.25(2)) \tag{3.1}$$

$$Length = (diameter(number\ of\ pipes\ in\ a\ row))$$
$$+ (0.5(number\ of\ pipes\ in\ a\ column - 1) \tag{3.2}$$
$$+ (0.25(2))$$

$$Reformer\ Surface\ Area$$
$$= 2(Length \times Height) + 2(Width \times Height) \tag{3.3}$$
$$+ 2(Length \times Width)$$

3.2 Heat loss to furnace walls

The first calculation was the heat loss calculation from the reformer walls to the surroundings. The inside of the walls was assumed to be the same temperature as the bulk temperature of the combusted fuel. It was treated as an overall heat transfer coefficient calculation, with heat transfer by conduction through the furnace wall, and by natural convection to the outside air, shown in *figure 5*.
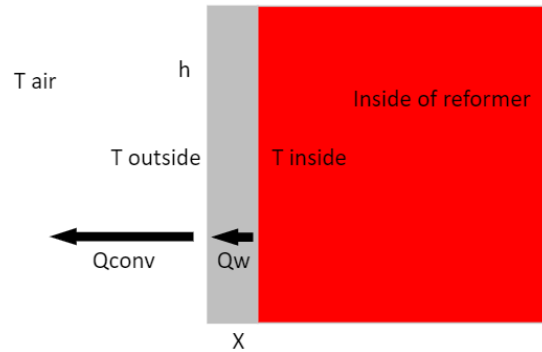
Figure 5: Heat flow from the reformer area to ambient surroundings

The rate of heat loss to surrounding was determined by calculating the the overall heat transfer coefficient, which first required the heat transfer coefficient for the natural convection. Where β is the thermal expansion coefficient of air, g is gravitational acceleration, T_o is the outside wall temperature, T_{air} is the ambient temperature of air, and ρ_{air}, μ_{air}, cp_{air} and k_{air} are the density, dynamic viscosity, specific heat capacity and thermal conductivity of air, respectively.

$$Gr = \frac{\beta_{air} g (T_o - T_{air}) l^3 \rho_{air}^2}{\mu_{air}^2} \qquad (3.4)$$

$$Pr = \frac{\mu_{air} Cp_{air}}{k_{air}} \qquad (3.5)$$

$$Nu = 0.13 (GrPr)^{0.33} \qquad (3.6)$$

$$h_{outside} = \frac{Nu \, k_{air}}{l} \qquad (3.7)$$

The overall heat transfer coefficient, U, was then used to calculate the rate of heat loss. Where x_{wall} is the wall thickness and $A_{surface}$ is the surface area of the reformer.

$$U = \frac{1}{\left(\frac{1}{h_{outside}} + \frac{x_{wall}}{k_{wall}}\right)} \qquad (3.8)$$

$$Q_{wall} = UA_{surface}(T_i - T_{air}) \qquad (3.9)$$

3.3 Heat loss to process pipes

The calculation of the heat transfer to the pipes uses the outside temperature of the pipe walls which was assumed to be the same temperature as the bulk temperature of the combusted fuel. On the inside of the pipes, forced convection takes place as the process fluid is moving through the pipe (*figure 6*). To account for the catalyst-packed pipes in a steam methane reformer, the pipes are made of 2 layers, one steel and one nickel alloy (NiO/Al$_2$O$_3$).
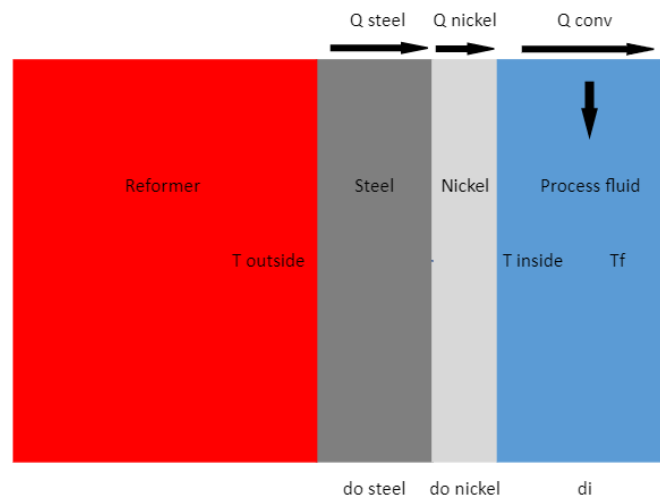
Figure 6: Heat flow from reformer furnace area to process fluid

The mixture properties used for this analysis were calculated by taking the properties of both steam and methane at the film temperature of the interior pipe wall and the bulk temperature of the mixture and using the S/C ratio.

$$mixture\ property$$

$$= \left(steam\ property\left(\frac{\frac{S}{C}ratio}{\left(\frac{S}{C}ratio\right)+1}\right)\right) \qquad (3.10)$$

$$+ \left(methane\ property\left(\frac{\left(\frac{S}{C}ratio+1\right)-\frac{S}{C}ratio}{\left(\frac{S}{C}ratio\right)+1}\right)\right)$$

The forced convection heat transfer coefficient was first calculated for 1 pipe.

$$\dot{m}_{one\ pipe} = \frac{\dot{m}_{total}}{number\ of\ pipes} \tag{3.11}$$

$$v = \frac{\dot{m}_{one\ pipe}}{\rho_{mixture} A_{inside}} = \frac{\dot{m}_{one\ pipe}}{\rho_{mixture}(\pi(\frac{d_i}{2})^2)} \tag{3.12}$$

$$Re = \frac{\rho_{mixture} v d_i}{\mu_{mixture}} \tag{3.13}$$

$$Pr = \frac{\mu_{mixture} Cp_{mixture}}{k_{mixture}} \tag{3.14}$$

$$Nu = 0.0225\ Re^{0.8}\ Pr^{0.33} \tag{3.15}$$

$$h_{inside} = \frac{Nu\ k_{mixture}}{d_i} \tag{3.16}$$

The overall heat transfer coefficient, U, was then calculated using the pipe layer properties.

$$U = \frac{1}{\left(\frac{1}{h_{inside}} + \frac{(d_{o\ steel} - d_{o\ nickel})}{k_{steel}} + \frac{(d_{o\ nickel} - d_i)}{k_{nickel}}\right)} \tag{3.17}$$

As the reaction taking place in the reformer pipes is endothermic, the additional energy absorbed by the mixture had to be considered. For this reaction, the change in enthalpy, Δh_{endo}, is equal to 206.2 kJ/mol$_{CH4}$, so the additional energy loss was calculated using the molar flow of methane.

$$Q_{endothermic} = \Delta h_{endo}(molar\ flow\ rate\ of\ methane) \tag{3.18}$$

This energy loss was combined by the heat transfer rate to obtain the total amount of energy loss to the pipes.

$$Q_{pipe} = UA_{surface}(T_{outside} - T_{mixture}) \tag{3.19}$$

$$Q_{total} = (Q_{pipe}(number\ of\ pipes)) + Q_{endothermic} \tag{3.20}$$

3.4 Fuel Requirements

In order to calculate how much fuel would be needed to supply the same rate of energy as the total heat loss, the lower heating value of the fuel had to be calculated. Since the only combustible properties in the fuel mixture are hydrogen and methane, the lower heating value of these components was used with their percentage of mixture composition to calculate the LHV of the mixture. The composition of the fuel mixture being fed to the burners was sourced through a CFD study of an industrial-scale SMR [20]. This composition is shown in *table 2*.

Table 2: Composition of fuel mixture before combustion [20]

	H20	O2	Ar	N2	H2	CO2	CO	CH4
Composition (%)	0.0039	0.161	0.0071	0.6008	0.0592	0.0972	0.0208	0.0501
Molar mass (kg/mol)	0.018	0.032	0.0399	0.028	0.002	0.044	0.028	0.016
Total mass (kg/mol)	0.028107							

The required fuel was then calculated as follows.

$$Q_{total} = Q_{pipes} + Q_{wall} \tag{3.21}$$

$$LHV_{mixture} = (molmass_{H2}LHV_{h2}) + (molmass_{CH4}LHV_{CH4}) \tag{3.22}$$

$$Fuel\ molar\ flow\ rate = \frac{Q_{total}}{LHV_{mixture}} \tag{3.23}$$

$$
\begin{aligned}
&Fuel\ mass\ flow\ rate \\
&= Required\ molar\ flow\ rate\ (Total\ molar\ mass\ of\ fuel)
\end{aligned}
\tag{3.24}
$$

$$
\begin{aligned}
&Hydrogen\ fuel\ molar\ flow\ rate \\
&\qquad = fuel\ flow\ rate \times composition_{H2}
\end{aligned}
\tag{3.25}
$$

$$
\begin{aligned}
&Methane\ fuel\ molar\ flow\ rate \\
&\qquad = fuel\ flow\ rate \times composition_{CH4}
\end{aligned}
\tag{3.26}
$$

3.5 Head Loss from Friction

An important associated with reformer design is the head loss in the pipes due to friction. This accounts for an increase in fluid velocity when the design of the reformer is altered. The head loss due to friction (m) was calculated using the Darcy-Weisbach equation.

$$h_f = f \, \frac{l_{pipe} v^2}{2Dg} \qquad \textbf{(3.27)}$$

Where f is the friction factor, l_{pipe} is the length of the reformer pipes (m), v is the flow velocity in one pipe (m/s), D is the internal diameter of the pipe (m), and g is the gravitational acceleration constant (m/s^2). The friction factor was calculated using the Moody chart which correlates the Reynolds number and relative roughness in a pipe to the friction factor. Relative roughness is calculated using the following equation.

$$Relative\ Roughness = \frac{absolute\ roughness}{D} \qquad \textbf{(3.28)}$$

Where absolute roughness (m) is a constant associated with the pipe material. The head loss value was used to calculate the pump power required to overcome the head loss.

$$P_{pump} = h_f \cdot g \cdot \dot{m}_{mixture} \qquad \textbf{(3.29)}$$

Where $\dot{m}_{mixture}$, is the total mass flow rate of the methane-steam mixture through the reformer.

3.6 Contact time

As well as friction, another important consideration in the reformer time is contact time. As the reaction in the reformer pipes is catalytic, there would be a minimum contact time needed for the mixture on the catalyst, to ensure a complete reaction. This contact time was calculated by volume, V, and volumetric flow rate, $\dot{V}$.

$$Contact\ time = \frac{V}{\dot{V}} \qquad\qquad (3.30)$$

$$\dot{V} = vA = v(\pi(\frac{D}{2})^2) \qquad\qquad (3.31)$$

Where v is velocity in a pipe and A is the cross-sectional area of the pipe.

3.7 Compressor power

Another energy expense in the system is the compression of methane before the reforming stage. The compression was assumed to be isentropic, therefore, the power was calculated using the temperatures at both sides of the compressor, T_1 and T_2, the specific heat capacity of methane at ambient temperature, C_p, and the mass flow rate of methane $\dot{m}_{CH4}$.

$$P = c_p(T_2 - T_1)\dot{m}_{CH4} \qquad\qquad (3.32)$$

3.8 Steam Heat Exchangers

The internal energy of the steam used in an SMR plant is a relevant energy input when assessing efficiency. Most SMR plants, however, generate their steam by feeding water through heat exchangers containing the hot fluids from different parts of the plant such as furnace fuel output and reformate output. In order to assess if these heat exchangers would provide enough energy for to generate steam at the correct temperatures, a calculation was added to the model which calculates the outlet temperature of the steam, by assuming a heat exchanger efficiency of 90%. The steam for the reformate, must be 600°C, so if this was not achievable by the heat exchangers, the energy required to further increase the temperature would be calculated and added to the efficiency calculation. For a heat exchanger that uses the outlet reformate as a heat source:

$$T_{steam\ out} = \frac{\varepsilon C_{min}(T_{reformate\ in} - T_{steam\ in})}{C_{steam}} + T_{steam\ in} \qquad\qquad (3.33)$$

$$C = \dot{m}c_p \qquad\qquad (3.34)$$

$$C_{min} = \min\left(C_{steam}, C_{reformate}\right) \quad \text{(3.35)}$$

Where ε is the effectiveness of the heat exchanger, T is the temperatures at the inlets or outlets, c_p is the specific enthalpy of a fluid at its inlet temperature and $\dot{m}$ is the mass flow rate.

3.9 Efficiency

The overall efficiency of the system was calculated by using the total energy into the system and the total energy out.

$$Efficiency = \frac{E_{out}}{E_{in}} \quad \text{(3.36)}$$

The total energy out of the system is equal to the hydrogen energy produced minus the hydrogen used in the reformer fuel, where $\dot{m}_{H2}$ is the mass flowrate of the output hydrogen, $\dot{m}_{h2fuel}$ is the mass flow rate of hydrogen used in fuel and LHV_{H2} is the lower heating value.

$$E_{out} = \dot{m}_{H2}LHV_{H2} - \dot{m}_{h2fuel}LHV_{H2} \quad \text{(3.37)}$$

Since the reformer fuel uses both added hydrogen and added methane for the combustion, the quantity of these components used in the fuel must be considered when analysing the efficiency. As the endothermic reaction in the reformer was considered while calculating the energy input, the exothermic reaction in the WGS reactor was calculated as it transfers energy back to the system. As the reformer reaction states that 1 mole of CO is produced by 1 mole of CH_4, the amount of energy released can be calculated using the molar flow rate of methane. Where Δh_{exo} is equal to 41.2 kJ/mol$_{CH4}$.

$$Q_{exothermic} = \Delta h_{exo}(molar\ flow\ rate\ of\ methane) \quad \text{(3.38)}$$

The total energy into the system comes from the input methane, the input energy required to generate the steam (if the heat exchangers cannot achieve this), minus the endothermic energy released in the WGS reactor reaction.

$$E_{in} = LHV_{CH4}(\dot{m}_{CH4} + \dot{m}_{fuelCH4}) + \dot{m}_{H2O}h_{H2O} - Q_{exothermic} \qquad \textbf{(3.39)}$$

Therefore, the total efficiency of the system is calculated as follows.

$$Efficiency = \frac{\dot{m}_{H2}LHV_{H2} - LHV_{H2}(m_{fuelH2}) +}{LHV_{CH4}(\dot{m}_{CH4} + \dot{m}_{fuelCH4}) + \dot{m}_{H2O}h_{H2O} - Q_{exothermic}} \qquad \textbf{(3.40)}$$

3.10   Analysis

The mathematical model was used to conduct sensitivity analyses, showing the effects of varying parameters on the overall efficiency of the system. The 4 factors studied in the analysis were, number of pipes in the reformer, pipe length, pipe diameter, and mass flow rate. Each analysis was conducted for all 3 yield cases shown in *table 3*, to obtain a range of potential system efficiencies. The studies began by simulating the model at the baseline configuration and then adjusting the values of their respective variables. results were recorded by plotting several variables from each iteration on Excel.

Table 3: Baseline parameters of reformer model

Variable	Units	Value	Source
Molar flow rate	mol/s	2233.33	[15]
Mass flow rate	kg/s	39.08	Calculated
Ait temperature	K	298.15	Assumed
Outside wall temperature of reformer	K	673.15	Assumed
Inside wall temperature of reformer	K	1343.15	[15]
Reformer height	m	12.5	[20]

Thermal conductivity of reformer walls	W/mK	2.6	[20]
Wall thickness	m	0.15	[21]
Outside pipe wall temperature	K	1343.15	[15]
Inside pipe wall temperature (bulk)	K	973.15	Calculated
Inside diameter of reformer pipe	m	0.126	[15]
Outside diameter of catalyst layer	m	0.146	[15]
Outside diameter of steel layer	m	0.186	Assumed
Thermal conductivity of catalyst layer	W/mK	33	[15]
Thermal conductivity of steel layer	W/mK	29.5	[15]
Absolute roughness of inside pipe wall	m	0.00003	[22]

3.10.1 Number of pipes

The number of pipes in the reformer was decreased to examine its effects on the efficiency. Decreasing the number of pipes affects the geometry of the reformer in the model by lowering the surface area and the subsequent heat loss across the reformer walls. With less pipes, however, the velocity is increased as there is a greater share of the mass flow rate per pipe. With an increase in velocity, the required pump power to overcome friction increases

and the contact time of the mixture on the interior pipe would decrease. As mentioned in *Section 2.4 reformer*, traditional steam methane reformers require a contact time of no less than 1 second, so assuming this condition would limit the ability to decrease the number of pipes.

3.10.2 Pipe length
The second analysis involved decreasing the pipe length on the reformer. While this would have no effect on the friction factor of the pipe it would impact the head loss as it is a function of pipe length, as seen in the Darcy-Weisbach equation as well as lowering the contact time. Another affected factor in this change would be the heat loss to both the pipes, and the walls as the reformer height is equal to the length of the pipes.

3.10.3 Pipe Diameter
Out of all the factors examined, a change in pipe diameter would alter the required pump work the most, as the friction factor in being affected by both the Reynolds number and the diameter. The pipe diameter would also have an effect on both heat loss scenarios.

3.10.4 Mass flow rate
In an effort to examine the effects of scaling up a SMR plant, the mass flow rate of the mixture was increased, which would raise the hydrogen output of the plant. The pump power, heat loss to the pipes, and the contact times in the pipes would all be affected by this as they are a function of the mass flow rate. The mass flow rate of the system would also increase the required compressor work for methane.

4.0   Results and Discussion

The analysis was carried out for each variable discussed for all three yield cases shown in *table 1*.

4.1 Baseline

The base case was simulated to get a gauge of the efficiencies and energy inputs for the original design. The efficiencies of these case are shown on the chart in *figure 7*.

Efficiencies of Each case at Baseline Parameters
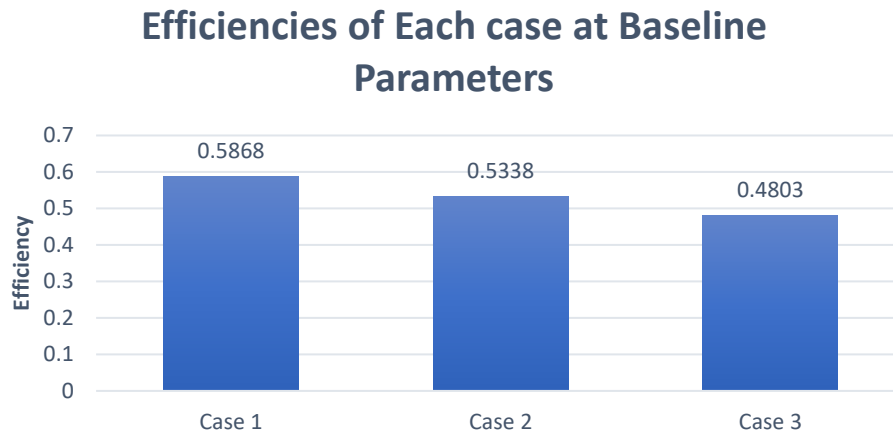
Figure 7: Efficiency values of each yield case at baseline parameters

As would be expected, the efficiency of each case goes in descending order from 1 to 3 as case 1 had the highest hydrogen yield at an S/C ratio of 3, and case 3 had the lowest yield with a higher S/C ratio of 3.2. The efficiency of the plant at baseline conditions ranged from 48.03-58.68%. It should also be noted that the steam heat exchanger in the model were successfully able to heat the steam to 600°C, which negated the need for additional heat energy and subsequently increased the efficiency compared to a scenario where no heat exchangers were considered. To demonstrate this the simulation was also carried out by adding the required heating energy for the steam to the efficiency calculation (*figure 8*).

Efficiencies with No Heat Exchanges
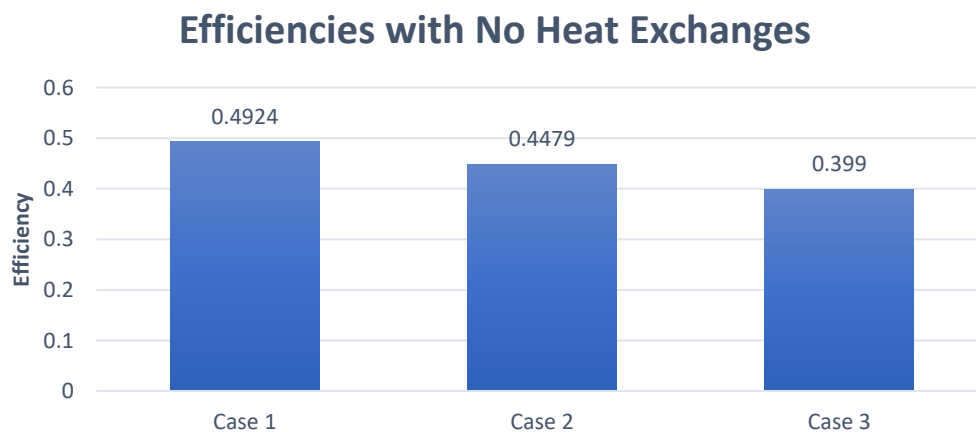
Figure 8: Efficiency values of baseline parameters with heat exchangers removed

Figure 8 shows that by not accounting for heat exchangers, the efficiency range for the plant decreased by an average of 8.72% across all three cases. The majority of the energy going into the system is from the chemical energy of methane (around 91.56%), as shown in *figure 9*. The pump work due to friction in the reformer is fairly insignificant in this configuration, only making up around 0.01%, however, this percentage may during the sensitivity analysis.

Distribution of Energy Into the System
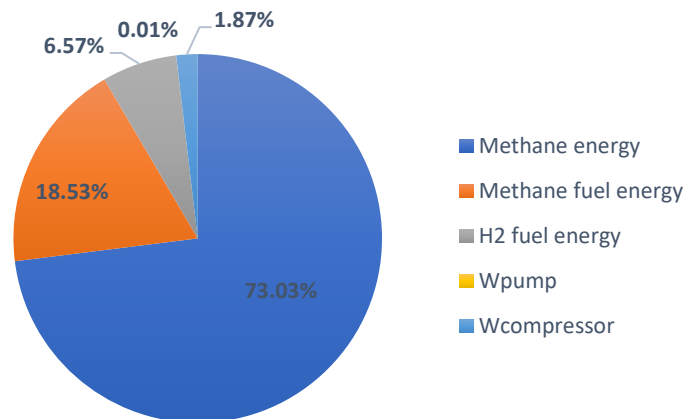
Figure 9: Percentage split of energy inputs to the SMR system

4.2 Number of pipes

The number of pipes was decreased from its original value of 336. As the number of pipes effects the layout of the reformer, the number of pipes per row and column also had to be changed, for example, for 250 pipes, the layout was adjusted to 25 x 10 pipes. Due to an increased Reynolds number when decreasing the amount of pipes, the friction factor had to be recalculated each iteration. This was done using a Moody chart calculator [23]. The number of pipes simulated for each case were 336 (baseline), 250, 150, 50 16, 9, 3, and 1. The effects of these changes are shown in *figure 10*.

Efficiency with Varying Number of Pipes
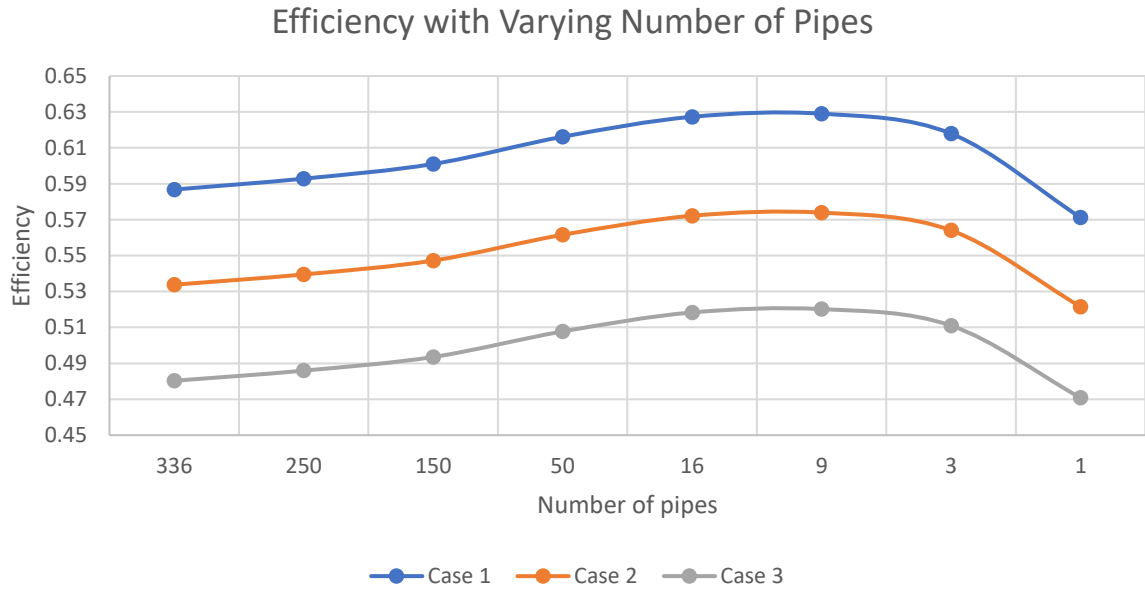
Figure 10: Effects of pipe number on efficiency, analysed at each yield case

Lowering the number of pipes initially increased the efficiency of the system, before reaching a maximum range of around 52-63% at around 11 pipes. This trend can be explained by examining the change in energy losses throughout the varying number of pipes, shown in *figure 11*. The figure shows the energy losses from reformer walls and the reformer pump in each interaction for case 1. As the number of pipes initially decrease the heat loss from the reformer walls decrease due to the reducing surface area, without much increase in the frictional head loss. However, after the number of pipes is reduced to under 16, the head loss increases exponentially due to a large increase in velocity per pipe.

Energy Losses from Decreasing Number of Pipes
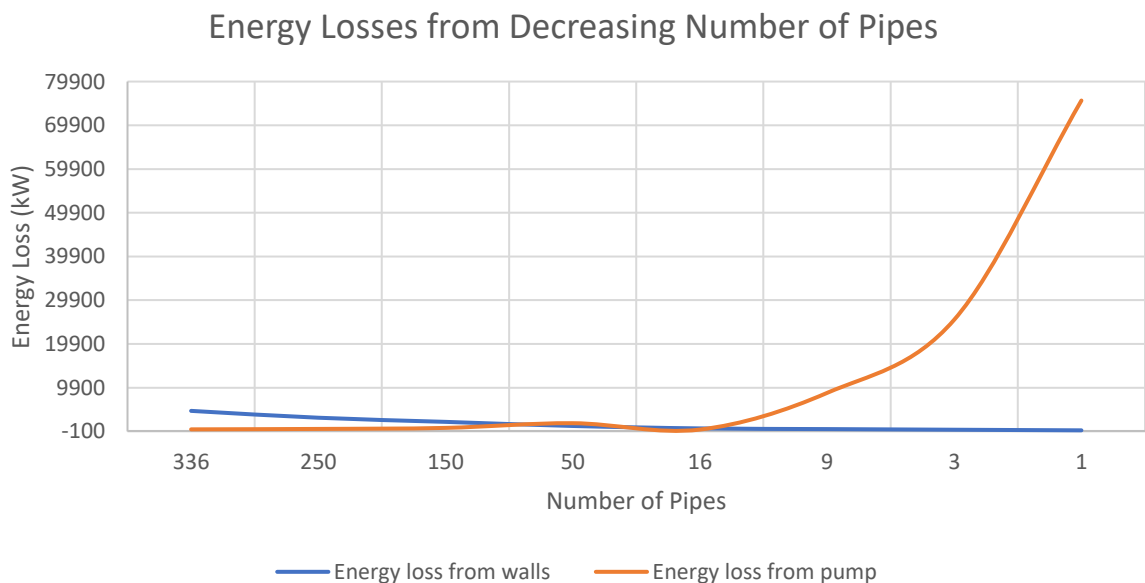
Figure 11: Rate of energy loss change with number of reformer pipes

Due to the drastic increase that resulted from the decreased number of pipes, the contact time for each of these configurations was recorded. Shown on *figure 12*, is the efficiency graph with the added contact time associated with each pipe amount simulated. Assuming the SMR reaction requires at least 1 second of contact time for a complete reaction, the graph highlights the threshold for which the contact time reaches 1 second. The maximum achievable efficiency ranges from decreasing the number of pipes is, therefore, around 49.5-60.5% at 130 pipes.
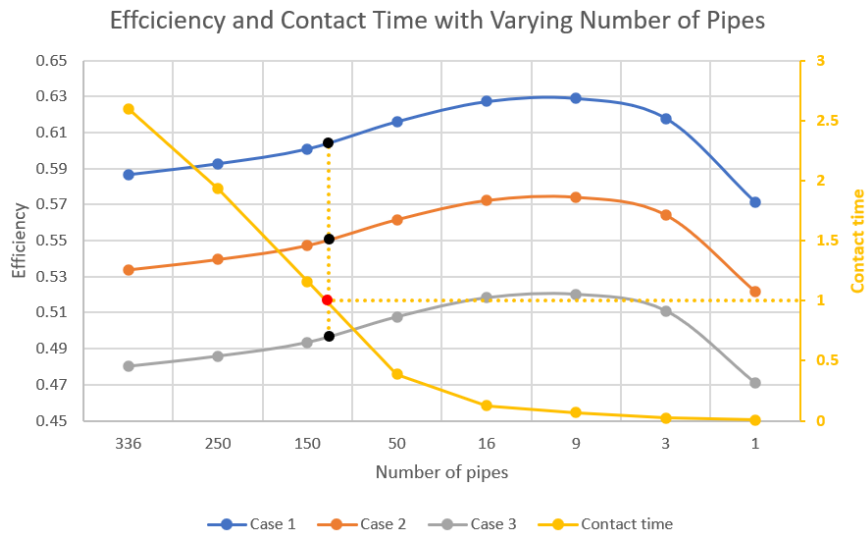
Figure 12: Efficiency values for number of pipes with added contact time, highlighting the points of maximum efficiency at 1 second

4.3 Pipe Length

The pipe lengths were tested at values of 15, 12.5 (baseline), 10, 7.5, 5, and 2.5 metres. As the internal diameter of the pipe and velocity of the fluid were constant in this analysis the friction factor did not have to be recalculated. The effects of pipe length on the energy losses in the reformer are shown in *figure 13*.
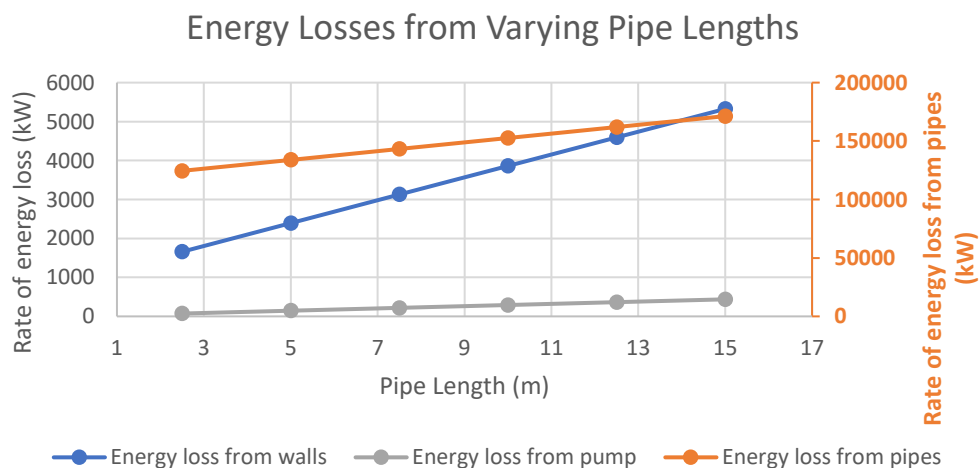
Figure 13: Rate of energy loss change with pipe length

As *figure 13* shows, increasing pipe length increases the energy loss from the pipes, walls and pump, linearly. It is for this reason that the overall efficiency of the system decreases linearly with the pipe length, as shown in *figure 14*.
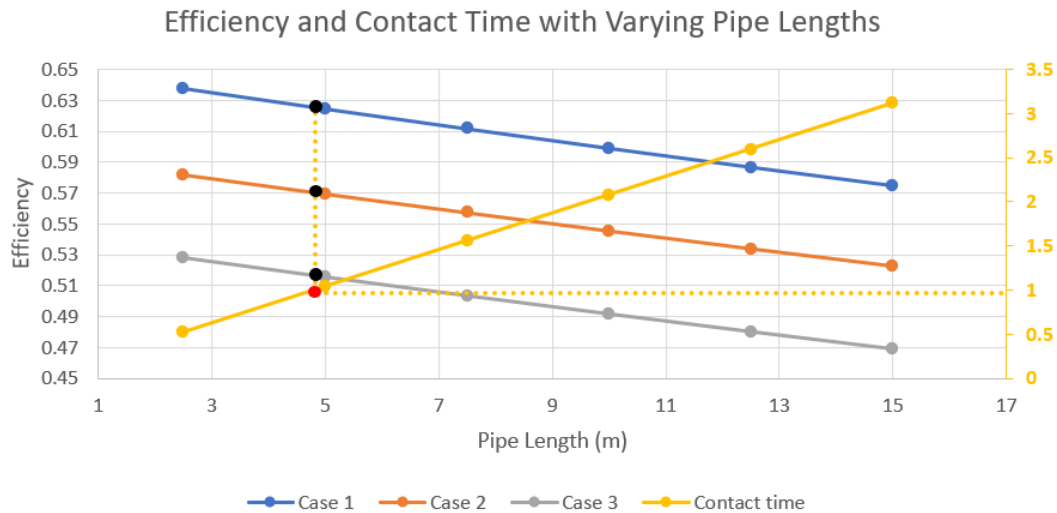
Figure 14: Efficiency values for pipe length with added contact time, highlighting the points of maximum efficiency at 1 second

Increasing the pipe does however increase the contact time of the mixture, as can be seen in *figure 14*, where, for the baseline mass flow rate, the length must be at lease around 5 metres to achieve a contact time of 1 second. Decreasing the length of the pipe to 5 m increases the efficiency range to around 51.6-62.5%. It is also worth noting that while an increase in pipe length negatively affected the efficiency in this scenario, its impact on contact time, means that this would be a good variable to explore when increasing the production of the plant, as this would counteract the loss in contact time from an increased mass flow of reactant mixture.

4.4 Pipe Diameter

Pipe diameter was tested at values of 0.05, 0.075, 0.1, 0.126 (baseline), 0.15, 0.175 and 0.2 metres. As the pipe diameter effects both the relative roughness and Reynolds number of the pipe, the friction factor was recalculated for each sized pipe. As length of the pipe did not change, the surface area of the reformer walls remained the same, and therefore, the heat loss to the walls was constant. The rate of energy loss to the pipes and to the reformer pumps were, however, affected by varying pipe sizes. The rate of energy loss for these factors are shown in *figure 15*.
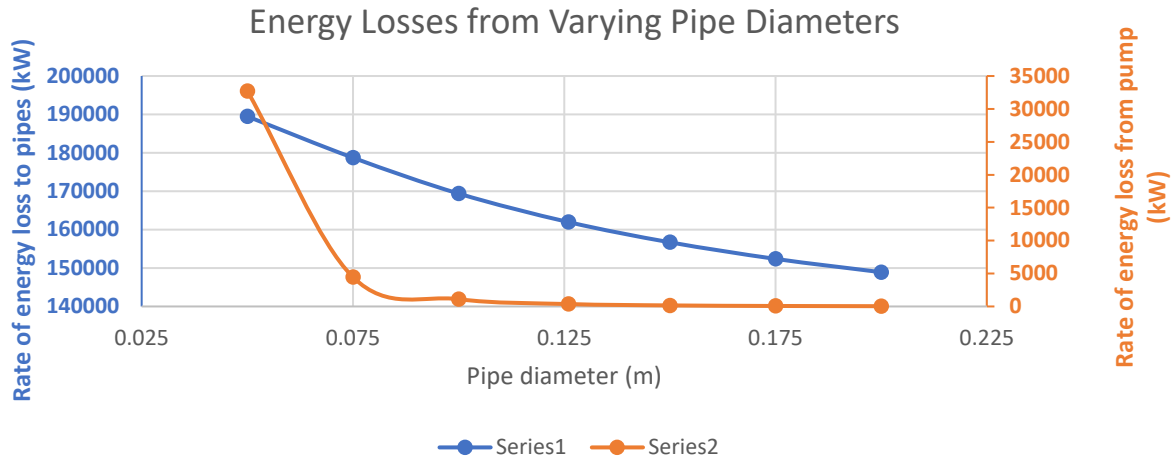
Figure 15: Rate of energy loss change with pipe diameter

The rate of heat transfer through the reformer pipes decreases exponentially as the pipe diameter increases. This is due to the reduction of fluid velocity as the pipe diameter increases. The required pump power for the reformer increases steadily as the pipe size is reduced, but starts to spike at a diameter of 0.025 m. As the frictional head loss and subsequent pipe power increase with higher velocities and smaller diameters, the values increase exponentially. The efficiency and contact time at each pipe diameter is shown in *figure 16*.
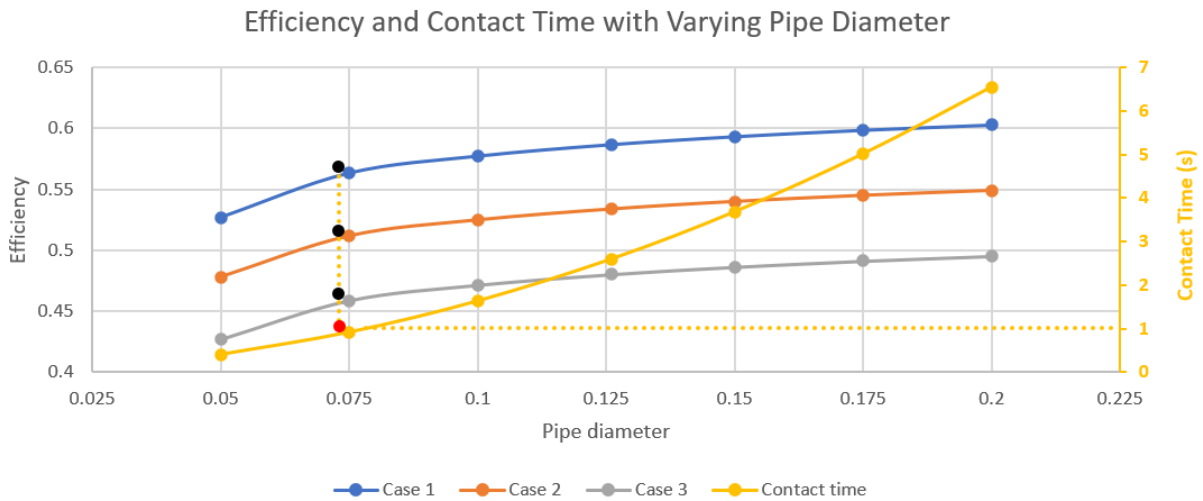
Figure 16: Efficiency values for pipe diameter with added contact time, highlighting the points of maximum efficiency at 1 second

As the head loss from friction and heat transfer rate through the pipes both increase with a smaller diameter, the efficiency decreases. Additionally, the contact time, as shown. Reaches 1 second around 0.075 m. While decreasing pipe diameter had no advantages to the system,

increasing the pipe diameter, would be another parameter to examine when increasing mass flow rate, as this would lower the velocity and its associated losses.

4.5 Mass Flow Rate

The mass flow rate was increased from the original value to analyse the how scaling up production effected efficiency. The values simulated were 39.08 (baseline), 52.5, 87.5, 131.25, 175, 218.75, 262.5, 350, 437.5, and 525 kg/s. These flow rates were tested for all three yield cases, and the friction factor was recalculated each time. Shown in *figure 17* is the energy losses as well as the hydrogen energy produce as the mass flow increases.
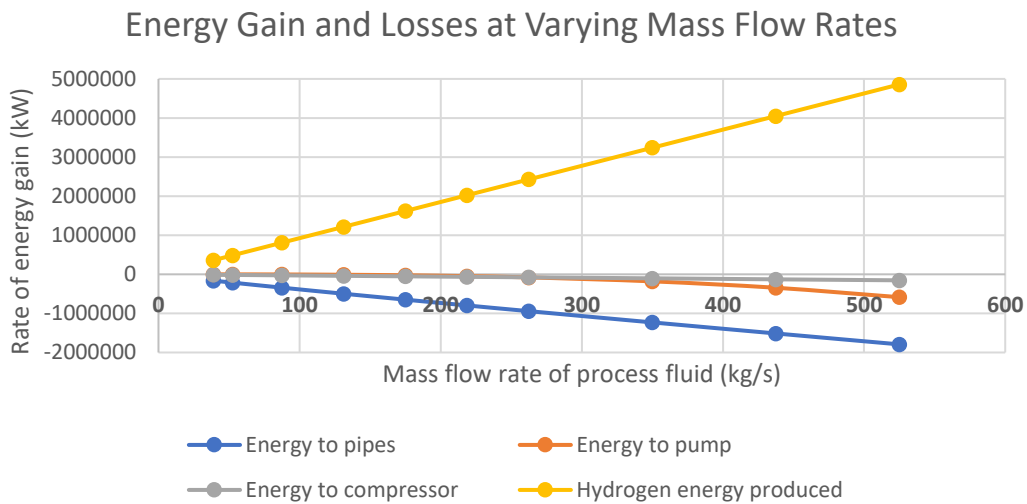
Figure 17: Rate of energy loss change with mass flow rate

The energy loss to the pipes, pump and compressor all increase with the mass flow rate, with the loss to the pump increasing exponentially as a result of the increasing pipe velocity. Additionally, the hydrogen energy output increases linearly with mass flow rate. The effects of these energy losses on the efficiency are shown below in *figure 18*.
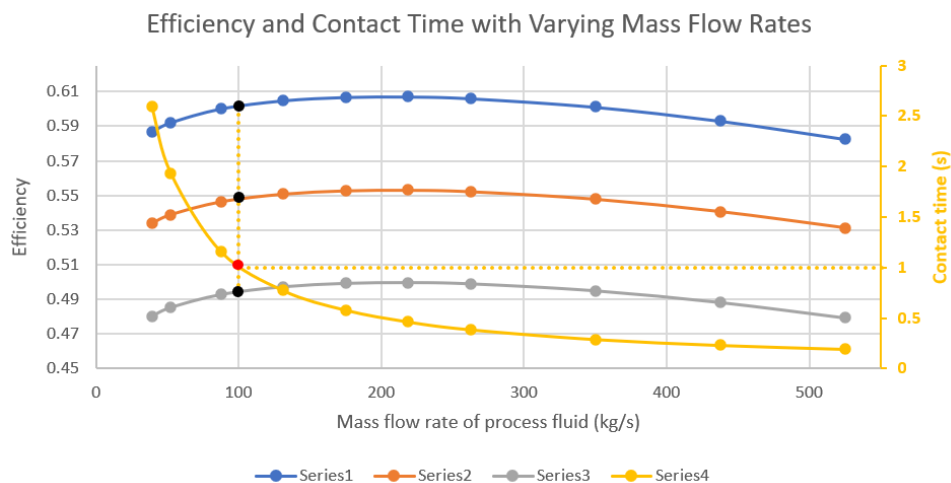
Figure 18: Efficiency values for pipe diameter with added contact time, highlighting the points of maximum efficiency at 1 second

Increasing the mass flow rate boosts the efficiency until a flow rate of around 200 kg/s. This is because the rate of which the energy losses increase is low up to this point, therefore, the ratio of hydrogen energy produces to energy lost steadily increases. After this point, however, the value of energy loss increases at a higher rate, which then reduces this ratio and consequently, the efficiency of the system. The contact time is the pipes is also affected by the flow rate, falling below 1 second after a flow rate of 100 kg/s. Assuming a 1 second requirement, the maximum achievable efficiency range for increasing the flow rate on the original reformer design is around 49.3-60.1% at a mass flow rate of 100 kg/s.

4.6 Improving Efficiency

With the correlations identified from the analysis, the model with multiple variables which were different from the baseline, to improve the maximum efficiency. Since the mass flow rate through the system governs the size requirement, this was kept constant, and the focus was to increase the efficiency of for the initial flow rate. To reduce head loss, the pipe diameter was increased. The length of the pipe was kept at a constant as changing its size would either increase head loss or reduce contact time. As increasing the diameter would demand more surface area in the reformer, the and the number of pipes was decreased to counteract this increase of surface area and minimise heat loss from the reformer walls. This analysis was only carried out for yield case 1 as it had the most efficiency out of all three. The designs simulated to increase efficiency are shown in *table 4*.

Table 4: Adjusted parameters for each new design configuration

Design	Number of Pipes	Diameter of Pipes (m)
Baseline	336	0.126
Design 1	120	0.2
Design 2	60	0.3
Design 3	30	0.4
Design 4	10	0.5
Design 5	5	0.6

As shown in *table 4*, the number of pipes and diameter was scales down to see the effects on the efficiency. The variables not listed in the table were all kept at the same value as the baseline design. The efficiency and contact time of each design is shown in *figure 19*.
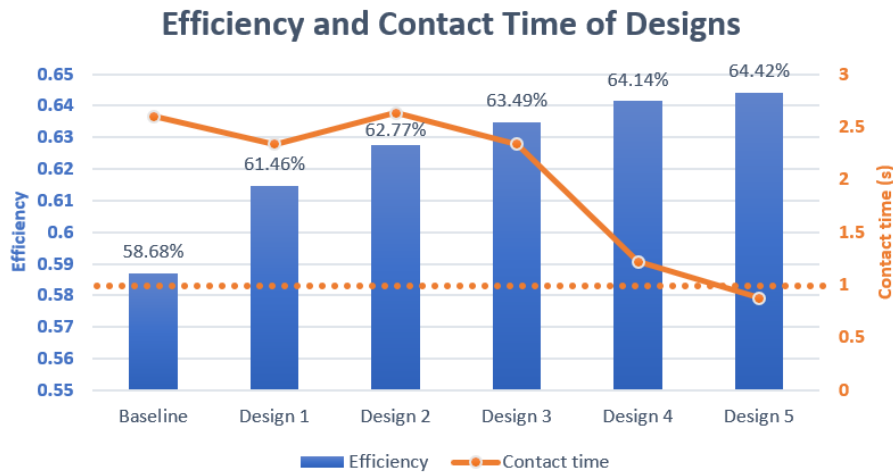
Figure 19: Efficiency and contact times from each design

As each design each design respective design change its number of pipes and pipe diameter more increasingly from the baseline, a consistent increase in efficiency. The contact times between each design did not reduce consistently as the two variables which were reduced, were not does in a proportional manner to each other. The highest efficiency achieved was by *Design 5* at 64.42%, however, the contact time achieved by this configuration was under 1 second, making it unsuitable. The best design was, therefore, *Design 4* as it achieved an efficiency of 64.14% and a contact time of 1.22 seconds. This value is similar to that given in the exergy analysis paper [17], which reached 66.65%. Although the efficiency achieved in this study was lower, this could have reached the same value, had it not been restricted by the 1 second contact time parameter, which the paper did not mention.

5.0   Future Work

While the model used for the analysis helped identify correlations between the system efficiency and values of several variables, some of the simplifications made may have caused inaccuracies in the results. Firstly, since most of the energy inputs into an SMR system revolve around the reformer stage (the main focus of the model), both the WGS, PSA and carbon capture stages, still consume energy in a real system, as shown in the exergy study [17]. The model would, therefore, have been more accurate had these systems also been incorporated.

An important area which affects the efficiency of SMR plants is both the temperatures and pressure values used, which is what many studies focus on. The method used for this model, however, would not have been compatible with a steam and pressure analysis since these factors directly affect the chemical kinetics of the reactions. Contrastingly, this analysis relied on a range hydrogen yield values given from studies which do consider these kinds of factors.

Another significant assumption made in the model was how it handled the nickel catalyst in the reformer pipes. The pipes in SMR systems are filled with catalyst particles to increase the surface area which the process fluid can be in contact with. This simplified the catalyst area by setting the inside of the pipe wall as catalyst material to try and account for its heat transfer coefficient during the heat loss calculation. From a technical standpoint, these two layouts would behave very differently with the flow through the pipe. This simplification is apparent in Section *4.6: Increasing Efficiency*, where the efficiency of the system increased with the pipe diameter. While this change lowered the head loss of the flow, increasing pipe diameter decreases pressure and the subsequent flow velocity. This is a relevant issue as a pipe packed with particles would provide more resistance to the fluid flow than one that is assumed empty, therefore, said pipe would likely require a larger differential pressure in order to overcome the flow resistance. Had this consideration been implemented in the model it would likely have yielded different results.

Future work could use this model to aid an overall supply chain analysis for hydrogen, which would also consider storage, transport, use and alternative production options, such as autothermal reforming and electrolysis.

As an energy plants design is influenced by economic as well as technical factors, an element of financial analysis would have been beneficial for the findings of this study. For example, expenses and profits could have been modelled using energy and resource market prices to

estimate a payback time for a given scale of plant, with an initial investment cost. Additionally, there are financial consideration associated with scaling up the production of a plant, due to the potentially increased material and fuel costs. This would have provided more insight into the considerations required when designing a SMR plant.

6.0   Conclusion

The phase-out of fossil fuels in now vital ahead of the 2050 emissions targets. With the UKs planned hydrogen strategy, blue hydrogen will play a big role in decarbonising the grid, with fossil fuel plants being repurposed for a cleaner energy production. This strategy will help support even cleaner methods of hydrogen production in the long term, such as electrolysis. To help achieve these targets, it is crucial that blue hydrogen is integrated in a responsible way, with rigorous research and development of carbon capture technology. With the amount of scepticism being met with the concept of blue hydrogen, energy companies may be held accountable for any shortcuts made which result in additional emissions which have not been acknowledged.

This project highlights some of the key technical factors of the reforming process that must be considered when evaluating the design of an SMR plant. The values used in this analysis were based on that of existing studies for a baseline design. The original design at these baseline conditions had a maximum efficiency of 58.68%, However, after applying the findings from the sensitivity analysis, this was increased to eventually achieve an efficiency of 64.14% with a catalyst contact time of 1.22 seconds. As seen from *Design 5*, the efficiency continued to go higher with increased changes, however, became unsuitable due to the assumed required contact time of 1 second. Despite this, assuming the development of SMR technology, such as the implementation of microchannel reactors, this required contact time could decrease dramatically to around 900 μs, allowing for greater opportunity to optimise the efficiency of the system.

The mass flow rate sensitivity analysis shows that scaling up production of a plant requires many technical considerations in order to limit the increase of subsequent energy losses such as heat and friction. It has also been noted that the scaling up of production would also require financial considerations as more material would be required to support the elevated flow rates which the plant would have to work with.

The UK hydrogen strategy indicates that hydrogen could make up 20-35% of their total energy consumption by 2050 [3], so the execution of this plan must tackle technical uncertainties as transparently and thoroughly as possible if the future is to be net zero. An emphasis on methane emissions should be taken when considering blue hydrogen projects and its GPW should be measured on a 20-year basis.

7.0   References

[1]   BP, "Statistical Review of World Energy," BP, 2020. [Online]. Available: https://www.bp.com/content/dam/bp/business-sites/en/global/corporate/pdfs/energy-economics/statistical-review/bp-stats-review-2020-full-report.pdf.

[2]   Departmer for Buisiness, Energy & Industrial Strategy, "Digest of UK Energy Statistics (DUKES): renewable sources of energy - Capacity of, generation from renewable sources and shares of total generation (DUKES 6.2)," 2022. [Online]. Available: https://www.gov.uk/government/statistics/renewable-sources-of-energy-chapter-6-digest-of-united-kingdom-energy-statistics-dukes. [Accessed 28 July 2022].

[3]   Department for Buisiness, Energy & Industrial Strategy, "UK hydrogen strategy," 17 August 2021. [Online]. Available: https://www.gov.uk/government/publications/uk-hydrogen-strategy. [Accessed 09 June 2022].

[4]   J. C. Molburg and R. D. Doctor, "Hydrogen from Steam-Methane Reforming with CO2 capture," 30 June 2003. [Online]. Available: https://www.yumpu.com/en/document/view/29644616/hydrogen-from-steam-methane-reforming-with-co2-capture.

[5]   L. Barelli, G. Bidini, F. Gallorini and S. Servili, "Hydrogen production through sorption-enhanced steam methane reforming and membrane technology: A review," *Energy,* vol. 33, no. 4, pp. 554-570, 2008. [Online]. Available: https://www.sciencedirect.com/science/article/pii/S0009250916301531

[6]   S. Sircar, "Pressure Swing Adsorption," *Industrial & Engineering Chemistry Reasearch,* vol. 41, no. 6, p. 1389–1392, 2002. [Online]. Available: https://pubs.acs.org/doi/full/10.1021/ie0109758

[7]   R. W. Howarth and M. Z. Jacobson, "How green is blue hydrogen?," *Energy Science and Engineering,* vol. 9, no. 10, pp. 1676-1687, 2021. [Online]. Available: https://onlinelibrary.wiley.com/doi/full/10.1002/ese3.956

[8]   UN Enviroment Programme, "Global Assessment: Urgent steps must be taken to reduce methane emissions this decade," 6 May 2021. [Online]. Available:

https://www.unep.org/news-and-stories/press-release/global-assessment-urgent-steps-must-be-taken-reduce-methane. [Accessed 16 June 2022].

[9] M. C. Romano, C. Antonini, A. Bardow, V. Bertsch, N. P. Brandon, J. Brouwer, S. Campanari, L. Crema, P. E. Dodds, S. Gardarsdottir, M. Gazzani, G. J. Kramer, P. D. Lund, N. M. Dowell1 and E. Martel, "Comment on "How green is blue hydrogen?"," *Energy Sience & Engineering,* vol. 10, no. 7, pp. 1944-1954, 2022. [Online]. Available: https://onlinelibrary.wiley.com/doi/full/10.1002/ese3.1126

[10] R. W. Howarth, "Methane emissions from fossil fuels: exploring recent changes in greenhouse-gas reporting requirements for the State of New York," *Journal of Integrative Environmental Sciences,* vol. 17, no. 3, pp. 69-81, 2020. [Online]. Available: https://www.tandfonline.com/doi/citedby/10.1080/1943815X.2020.1789666?scroll=top&needAccess=true

[11] Y. Tan, W. Nookuea, H. Li, E. Thorin and J. Yan, "Property impacts on Carbon Capture and Storage (CCS) processes: A review," *Energy Conversion and Management,* vol. 118, no. 15, pp. 204-222, 2016. [Online]. Available: https://www.sciencedirect.com/science/article/pii/S0196890416302163?casa_token=jEpfb_QZizoAAAAA:X8ufH36Xsrw_a5eRBjVszkw2lVYC8lLJvksFCWAzxxc3WMXBd2NCKppTlkQir69pQF-itjZUZQ

[12] S. I. Plasynski, J. T. Litynski, H. G. McIlvried and R. D. Srivastava, "Progress and New Developments in Carbon Capture and Storage," *Critical Reviews in Plant Sciences,* vol. 28, no. 3, pp. 123-138, 2009. [Online]. Available: https://www.tandfonline.com/doi/full/10.1080/07352680902776440?casa_token=Wf-Vm7x4ClsAAAAA%3A8dmoo06X83drY9Ecrv2wTSyhvvm9r4gctWVN_uBM6KGwsSGw3hjJWBsKQG3_PAFp4DeDTpWGQUNi

[13] J. Pires, F. Martins, M. Alvim-Ferraz and M. Simões, "Recent developments on carbon capture and storage: An overview," *Chemical Engineering Research and Design,* vol.

89, no. 9, pp. 1446-1460, 2011. [Online]. Available:

https://www.sciencedirect.com/science/article/pii/S0263876211000554?casa_token=e

3zEemqp6JQAAAAA:fBorZxXTjukrAj_kv-crov2T8u6eF-
aPoZpppk0zlpZZSFA4epIHYMKbuNFiH27c04hFrjVnng

[14] M. Kanniche, R. Gros-Bonnivard, P. Jaud, J. Valle-Marcos, J.-M. Amann and C.
Bouallou, "Pre-combustion, post-combustion and oxy-combustion in thermal power
plant for CO2 capture," *Applied Thermal Engineering,* vol. 30, no. 1, pp. 53-62, 2010.
[Online]. Available:

https://www.sciencedirect.com/science/article/pii/S1359431109001471?casa_token=o

WlsqfP7iXkAAAAA:aSd6h6GWT2dNW9k8Xt-
xZlrxKNf7oIzV6h6XIOIE9hVQq4iYjwq_bGMpp90g3q_gdoH4pmqiVQ

[15] L. Laoa, A. Aguirrea, A. Trana, Z. Wua, H. Duranda and P. D. Christofides, "CFD
modeling and control of a steam methane reforming reactor," *Chemical Engineering
Science,* vol. 148, pp. 78-92, 2016. [Online]. Available:
https://www.sciencedirect.com/science/article/pii/S0009250916301531

[16] A. L. Y. Tonkovicha, B. Yanga, S. T. Perrya, S. P. Fitzgeralda and Y. Wang, "From
seconds to milliseconds to microseconds through tailored microchannel reactor design
of a steam methane reformer," *Catalysis Today,* vol. 120, no. 1, pp. 21-29, 2007.
[Online]. Available:
https://www.sciencedirect.com/science/article/pii/S0920586106004615

[17] A. P. Simpson and A. E. Lutz, "Exergy analysis of hydrogen production via steam
methane reforming," *International Journal of Hydrogen Energy,* vol. 32, no. 18, pp.
4811-4820, 2007. [Online]. Available:
https://www.sciencedirect.com/science/article/pii/S036031990700482X

[18] R. A. Wood, R. D. Boardman, M. W. Patterson and P. M. Mills, "HTGR-Integrated
Hydrogen Production via Steam Methane Reforming (SMR) Process Analysis," Idaho
National Laboratory, Idaho, 2010. [Online]. Available:
https://art.inl.gov/NGNP/INL%20Documents/Year%202010/HTGR-
Integrated%20Hydrogen%20Production%20via%20Steam%20Methane%20Reforming

%20(SMR)%20Process%20Analysis%20rev%200.pdf

[19] D. Pashchenko, "Thermodynamic equilibrium analysis of steam methane reforming based on a conjugate solution of material balance and law action mass equations with the detailed energy balance," *International Journal of Energy Research,* vol. 44, no. 1, pp. 438-447, 2019. [Online]. Available: https://onlinelibrary.wiley.com/doi/full/10.1002/er.4943

[20] A. Tran, A. Aguirre, H. Durand, M. Crose and P. D. Christofides, "CFD modeling of a industrial-scale steam methane reforming furnace," *Chemical Engineering Science,* vol. 171, pp. 576-598, 2017. [Online]. Available: https://www.sciencedirect.com/science/article/pii/S0009250917303901

[21] I. Jain, R. Singh and D. Mazumdar, "Measurements of Some Thermal Properties of Steel-Refractory Systems and Heat Losses from Steelmaking Furnaces," *Transactions of the Indian Institute of Metals,* vol. 68, no. 3, 2014. [Online]. Available: https://www.researchgate.net/publication/272748209_Measurements_of_Some_

Thermal_Properties_of_Steel-
Refractory_Systems_and_Heat_Losses_from_Steelmaking_Furnaces

[22] Neutrium, "ABSOLUTE ROUGHNESS OF PIPE MATERIAL," Neutrium, 19 May 2012. [Online]. Available: https://neutrium.net/fluid-flow/absolute-roughness-of-pipe-material/. [Accessed 14 July 2022].

[23] EngineerExcel, "MOODY CHART CALCULATOR," 2022. [Online]. Available: https://engineerexcel.com/moody-chart-calculator/. [Accessed 28 July 2022].

8.0 Appendix 1 – MATLAB model

```matlab
clear
clc

%%%%%%%%%%%%%%%%%%%%%%%%%%%%%%%%%%%%%%%%%%%%%%%%%%%%%%%%%%%%%%%%%%%%%%%%%
%heat loss to process gas pipes

%inputs
SC_ratio = 3; %steam to methane ratio
molm_mix = 2233.3; %molar flow rate of mixture (mol/s)
molmass_H20 = 0.018; %molar mass of water (kg/mol)
molm_H20 = ((SC_ratio/(SC_ratio+1))*molm_mix); %molar flow of steam (mol/s)
molmass_CH4 = 0.016; %molar mass of methane (kg/mol)
molm_CH4 = (((SC_ratio+1)-SC_ratio)/(SC_ratio+1))*molm_mix; %molar flow of methane
(mol/s)
m_CH4 = molm_CH4*molmass_CH4; %mass flow of methane (kg/s)
m_H20 = molm_H20*molmass_H20; %mass flow of steam (kg/s)
m_mix = m_CH4+m_H20; %mass flow of mixture (kg/s)

di = 0.126; %inside diameter of pipe (m)
di_steel = di+0.02; %inside diameter of steel layer (m)
do = di_steel+0.04; %outside diameter of pipe (m)
l_pipe = 12.5; %length of pipe (m)
k_steel = 29.5; %thermal conductivity of steel (W/mK)
k_nickel = 33; %thermal conductivity of nickel (W/mK)
T_outsidepipe = 1343.15; %average temp outside pipe (K)
T_insidepipe = 1273.15; %temperature on inside pipe wall (K)
T_mixin = 873.15; %inlet temperature of mixture(K)
T_mixout = 1073.15; %outlet temperature of mixture(K)
T_mixave = (T_mixin + T_mixout)/2; %average temperature of mixture(K)
T_filmpipe = (T_mixave + T_insidepipe)/2; %film temp (K)
c_H2O = 0.75; % mixture composition of steam (molH20/molmixture)
c_CH4 = 0.25; % mixture composition of methane (molCH4/molmixture)


cpH2O = 2217; %specific heat capacity of steam at film temp (J/kgK)
cpCH4 = 4214; %specific heat capacity of methane at film temp (J/kgK)
cpmix = (c_H2O*cpH2O) + (c_CH4*cpCH4); %cp of mixture (J/kgK)

den_H2O = 2.037; %density of steam at film temp (kg/m^3)
den_CH4 = 1.641; %density of steam at film temp (kg/m^3)
den_mix = (c_H2O*den_H2O) + (c_CH4*den_CH4); %density of mixture (kg/m^3)

vis_H2O = 4.41e-05; %dynamic viscocity of steam (kg/ms)
vis_CH4 = 3.13e-05; %dynamic viscocity of methane (kg/ms)
vis_mix = (c_H2O*vis_H2O) + (c_CH4*vis_CH4); %dynamic viscocity of mix (kg/ms)

k_H20 = 0.11967; %thermal conductivity of steam at film temp (W/mK)
k_CH4 = 0.1707; %thermal conductivity of methane at film temp (W/mK)
k_mix = (c_H2O*k_H20) + (c_CH4*k_CH4); %thermal conductivity of mix (W/mK)

dH_endothermic = 206200; %change in enthalpy due to endothermic reaction (J/mol)
Q_endothermic = dH_endothermic*molm_CH4; %energy absorbtion of reaction (J/S)
n_pipes = 336; %number of pipes
m_mixpipe = m_mix/n_pipes; %mass flow rate per pipe (kg/s)
A_surfin = pi*di*l_pipe; %inside surface area of pipe (m^2)
A_pipe = pi*(di/2)^2; %inside cross-sectional area of pipe (m^2)
v_mix = m_mixpipe/(den_mix*A_pipe); %velocity of mixture in pipe (m/s)
```

```matlab
Vol_mix = v_mix*A_pipe; %volumetric flow rate of mixture (m^3/s)
Vol_pipe = A_pipe*l_pipe; %volume of pipe (m^3)
t = Vol_pipe/Vol_mix; %contact time (s)

Re_pipe = (den_mix*v_mix*di)/vis_mix; %reynolds number
Pr_pipe = (vis_mix*cpmix)/k_mix; %Prandtl number
Nu_pipe = 0.0225*(Re_pipe^0.8)*(Pr_pipe^0.33); %nusselt number
hi = (Nu_pipe*k_mix)/di; %heat tranfer coefficient (W/m^2K)
Ui = 1/((1/hi)+(((di_steel-di)/2)/k_nickel)+(((do-di_steel)/2)/k_steel)); %overall
heat transfer coefficient (W/m^2K)

Q_pipe = Ui*A_surfin*(T_outsidepipe-T_mixave); %heat tranfer rate to pipe (W)
Q_totalpipes = (Q_pipe*n_pipes) + Q_endothermic; %heat tranfer rate to all pipes

%%%%%%%%%%%%%%%%%%%%%%%%%%%%%%%%%%%%%%%%%%%%%%%%%%%%%%%%%%%%%%%%%%%%%%%%%
%Heat loss to furnace walls

%inputs
T_air = 298.15; %temperature of air outside reformer (K)
T_outwall = 673.15; %temperature of outer wall (K)
T_filmwall = (T_air+T_outwall)/2; %film temp (K)
T_inwall = T_outsidepipe;

den_air = 0.727; %density of air at film temp (kg/m^3)
beta_air = 2.055e-3; %thermal expansion coefficient of air (1/K)
g = 9.81; %gravitational acceleration (m/s^2)
vis_air = 2.62e-5; %dynamic viscocity of air (kg/ms)
cp_air = 1028; %specific heat capacity of air (J/kgK)
k_air = 0.03901; %thermal conductivity of air (W/mK)

%heat transfer rate calculation
row_pipe = 7; %number of pipes in row
column_pipe = 48; %number of pipes in column
height = l_pipe; %height of reformer
width = (di*row_pipe)+(0.5*(row_pipe-1))+(0.25*2); %width of reformer (m)
length = (di*column_pipe) + (0.5*(column_pipe-1))+(0.25*2); %length of reformer
(m)
Gr_wall = (beta_air*g*(T_outwall-T_air)*height^3*den_air^2)/vis_air^2; %Grashof
number
Pr_wall = (vis_air*cp_air)/k_air; %prandtl number
Nu_wall = 0.13*(Gr_wall*Pr_wall)^0.33; %Nusselt number
ho = (Nu_wall*k_air)/height; %heat tranfer coefficient (W/m^2K)

x_wall = 0.15; %reformer wall thickness (m)
k_wall = 2.6; %Thermal conductivity of reformer wall (W/mK)
A_surwall1 = width*height; %surface area of wall 1 (m^2)
A_surwall2 = length*height; %surface are of 2 (m^2)
A_surwall3 = length*width;%surface are of 3 (m^2)
A_surTOT = (2*A_surwall1)+(2*A_surwall2)+(2*A_surwall3);
Uo = 1/((1/ho)+(x_wall/k_wall)); %overall heat transfer coefficient (W/m^2K)
Q_wall = (2*(Uo*A_surwall1*(T_inwall-T_air))) + 2*((Uo*A_surwall2*(T_inwall-
T_air))) + 2*((Uo*A_surwall3*(T_inwall-T_air))); %heat tranfer rate to
surroundings (W)

%%%%%%%%%%%%%%%%%%%%%%%%%%%%%%%%%%%%%%%%%%%%%%%%%%%%%%%%%%%%%%%%%%%%%%%%%
%Pump energy to overcome head loss
epsilon = 3E-05; %absolute roughness of pipe (m)
roughness = epsilon/di; %relative roughness of pipe
```

```matlab
f = 0.01410; %Friction factor, taken from Moody chart

hf = ((f*l_pipe*((v_mix)^2))/(2*g*di))*n_pipes; %head loss due to friction
W_pump = (m_mix*g*hf)/1000; %power to overcome head loss (kJ/s)

%%%%%%%%%%%%%%%%%%%%%%%%%%%%%%%%%%%%%%%%%%%%%%%%%%%%%%%%%%%%%%%%%%%%%%%%
%exothermic enrergy gained in WGS stage
dh_exothermic = 41200; %change in enthalpy due to exothermic reaction (J/mol)
Q_exothermic = (dh_exothermic*molm_CH4)/1000; %energy absorbtion of reaction
(KJ/S)

%%%%%%%%%%%%%%%%%%%%%%%%%%%%%%%%%%%%%%%%%%%%%%%%%%%%%%%%%%%%%%%%%%%%%%%%%%%%
%fuel requirment

molmass_H2 = 0.002; %molar mass of hydrogen (kg/mol)
molmass_CH4 = 0.016; %molar mass of methane (kg/mol)
molmass_fuel = 0.02810709; %molar mass of fuel (kg/mol)
H2_mol = 0.0592; %moles of hydrogen (molH2/molfuel)
CH4_mol = 0.0501; %moles of methane (molCH4/molfuel)
H2_LHV = 119988; %Lower heating value of H2 (kJ/kg)
H2_LHVmol = H2_LHV*molmass_H2; %Lower heating value of H2 (kJ/mol)
CH4_LHV = 50000; %Lower heating value of CH4 (kJ/kg)
CH4_LHVmol = CH4_LHV*molmass_CH4; %Lower heating value of CH4 (kJ/mol)
fuel_LHV = (H2_LHVmol*H2_mol) + (CH4_LHVmol*CH4_mol); %LHV of fuel (kJ/mol)

Q_total = (Q_totalpipes + Q_wall)/1000; %total rate of heat loss (kJ/s)
mol_fuel = Q_total/fuel_LHV; %required molar flow rate of fuel (mol/s)
m_fuel = mol_fuel*molmass_fuel; %required mass flow rate of fuel (kg/s)


%%%%%%%%%%%%%%%%%%%%%%%%%%%%%%%%%%%%%%%%%%%%%%%%%%%%%%%%%%%%%%%%%%%%%%%%%%%%
%Efficiency

H2_yeild = 2.7; %hydrogen yeild (molH2/molCH4)

molm_h2 = molm_CH4*H2_yeild; %Hydorgen output yeild (mol/s)
E_H2 = molm_h2*H2_LHVmol; %hydrogen energy output (kJ/s)

E_CH4 = molm_CH4*CH4_LHVmol; %energy input from hydrogen stream (kJ/s)

%heating of steam with PSA outlet Hydrogen heat exchanger
Effectiveness = 0.9; %assumed effectiveness of heat exchanger
T_steam1 = 298.15; %temperature of water at inlet to system (K)
cp_water = 4180; %specific heat capacity of water at temperature (J/kgK)

T_H2_1 = 723.15; %temperature of hydrogen at PSA outlet (K)
cp_H2_1 = 1462.315; %specific heat capacity of hydrogen at temperature (J/kgK)
m_H2 = molm_h2*molmass_H2; %mass flow rate of hydrogen (kg/s)

C_steam1 = m_H20*cp_water;
C_H2 = m_H2*cp_H2_1;
Cmin1 = min(C_steam1, C_H2);

T_steam2 = ((Effectiveness*(Cmin1*(T_H2_1-T_steam1)))/C_steam1) + T_steam1;

%heating of steam with PSA outlet Hydrogen heat exchanger
T_Refromate1 = 1073.15; %Temperature of reformate at outlet of reformer (K)
cp_reformate = 9851.1338; %Specific heat capacity of reformate (J/kgK)
m_reformate = m_mix; %mass flow rate of reformate
```

```matlab
cp_water2 = 4180;

C_steam2 = m_H20*cp_water2;
C_reformate = m_reformate*cp_reformate;
Cmin2 = min(C_reformate,C_steam2);

T_steam3 = ((Effectiveness*(Cmin2*(T_Refromate1-T_steam2)))/C_steam2) + T_steam2;

%energy use from fuel
mol_H2fuel = mol_fuel*H2_mol; %molar flow rate of hydrogen in fuel (mol/s)
mol_CH4fuel = mol_fuel*CH4_mol; %molar flow rate of methane in fuel (mol/s)

E_H2fuel = mol_H2fuel*H2_LHVmol;
E_CH4fuel = mol_CH4fuel*CH4_LHVmol;

%compressor work
T_CH41 = 298.15; %initial temperature of methane (k)
T_CH42 = 873.15; %Final temperature of methane (k)
cp_CH4_25 = 2226; %specific heat capacity of methane at ambient (J/kgK)
W_compressor = (cp_CH4_25*(T_CH42-T_CH41)*m_CH4)/1000;

%Steam energy with no heat exchangers
h_steam600 = 3698.1; %enthalpy of steam at 600 degrees (kJ/kg)
E_steam = h_steam600*m_H20; %internal energy of steam (kJ/s)

%overall efficiency
Efficiency = (E_H2-E_H2fuel + Q_exothermic)/((E_CH4 + E_CH4fuel + W_compressor +
W_pump));

table = table(di, l_pipe, m_mix, n_pipes, molm_mix, m_mixpipe, m_fuel, v_mix,
Re_pipe, A_surTOT, t, f, Q_wall, Q_totalpipes, W_pump, W_compressor, E_H2, E_CH4,
E_CH4fuel, E_H2fuel, Efficiency);
Results = rows2vars(table);

display (Re_pipe)
display (roughness)
```

Student No.